Robotica (2022), **40**, pp. 3651–3668
doi:10.1017/S0263574722000479

CAMBRIDGE UNIVERSITY PRESS

RESEARCH ARTICLE

UDE-based task space tracking control of uncertain robot manipulator with input saturation and output constraint

Yuxiang Wu, Fuxi Wan*, Tian Xu and Haoran Fang

School of Automation Science and Engineering, South China University of Technology, Guangzhou, Guangdong 510640, China
*Corresponding author. E-mail: 201920116459@mail.scut.edu.cn

Received: 1 April 2021; **Revised:** 9 January 2022; **Accepted:** 7 March 2022; **First published online:** 1 April 2022

Keywords: uncertainty and disturbance estimator, nonlinear state-dependent function, auxiliary system, robot manipulator

Abstract

This paper investigates the trajectory tracking problem of uncertain robot manipulators with input saturation and output constraints. Uncertainty and disturbance estimator (UDE) is used to tackle the model uncertainties and external disturbances. Different from most existing methods, UDE only needs the bandwidth of the unknown plant model for design, which makes it easy to be implemented. Nonlinear state-dependent function is employed to cope with output constraints and a second order auxiliary system is constructed to solve the input saturation. Finally, an UDE-based tracking controller is proposed based on the backstepping method. With the proposed control scheme, the input saturation and the output constraints are not violated, and all signals in the closed-loop system are bounded. The comparative simulation results of a two-link robot manipulator are utilized to validate the effectiveness and superiority of the proposed control method.

1. Introduction

The trajectory tracking control problem of robot manipulators has been extensively studied for the past decades, and lots of control schemes have been proposed in theory. As the robot manipulators are now required to have more physical interaction with humans and environment, many practical engineering problems, such as input constraints, output constraints, model uncertainties and external disturbances, cannot be ignored. Therefore, we need to design targeted controllers to deal with these problems.

In reality, the physical parameters of the robot manipulator are not always exactly known, which will greatly affect the control effect. Hence, many studies have been reported to solve this problem, such as neural network (NN) control [1, 2] and fuzzy logic system (FLS) control [3, 4]. Ling et al. [3] used FLS to approximate the dynamic uncertainties and updated FLS by updating the trace of the weight matrix transpose multiplied by the weight matrix. Similar to model uncertainties, external disturbances can also affect the control effect. To deal with this problem, a variety of disturbance observers (DO) have been constructed [5, 6, 7]. Shi et al. [5] designed a novel DO that can detect external disturbances and model uncertainties. Different from the complex designs of NN, FLS and DO, UDE is a simple designed filter, and only the bandwidth of the unknown object is required for the filter design [8], which makes the UDE-based control easier to be implemented and tuned. However, the above studies did not take the constraints into account.

With the increasing of man-machine cooperation scenarios, constrained control is essential to ensure the safety of operators. Lots of studies have been proposed to solve input constraints [9, 10, 11, 12] and output constraints [13, 14, 15, 16]. In ref. [9], a model predictive control method for robot manipulators based on NN was proposed, and non-quadratic cost functions were introduced to solve input constraints. In ref. [11], a fixed-time control method based on NN was presented for robot manipulators, and the NN was used to compensate the input dead zone. Tang et al. [13] proposed an adaptive neural tracking controller for robot manipulators, and solved symmetric output constraints by integral barrier Lyapunov

function (BLF). Compared with general BLF, NSDF proposed in ref. [16] is more concise and can solve both symmetric and asymmetric output constraints. However, most of the above studies are conducted in joint space.

Compared with the trajectory tracking control in joint space, the trajectory tracking control in task space is more practical. At present, there are two main methods to realize the trajectory tracking control of robot manipulators in task space. One method is to use the pseudo-inverse of the Jacobian matrix [17, 18, 19, 20, 21, 22]. Liu et al. [17] proposed an adaptive NN controller for robot manipulators with the optimal number of hidden nodes and less computation. In ref. [18], a repetitive learning controller for uncertain robot manipulators was designed to ensure high accuracy of tracking in task space. However, Liu et al. [17] and Dogan et al. [18] only considered the uncertain dynamics. Liang et al. [19] designed a TDE-based task space trajectory tracking controller for robot manipulators with uncertain kinematics and dynamics. Another method is to utilize the dynamic regressor matrix [23, 24, 25, 26, 27]. In ref. [24], an adaptive task space controller was proposed for robot manipulators with uncertain kinematics and dynamics, and the measurements of task space velocity and joint acceleration were avoided by introducing filters. Hanlei Wang [25] proposed two adaptive controllers for robot manipulators to realize the task space trajectory tracking control with uncertain kinematics and dynamics. Hu et al. [26] presented an adaptive task space trajectory tracking controller for space robot manipulators, and the model uncertainties and external disturbances with unknown bound were both considered.

Inspired by the above research, considering the input saturation and output constraints, an UDE-based tracking controller for uncertain robot manipulators with external disturbance is designed in task space. The model uncertainties and external disturbance are approximated by UDE, and the input saturation and output constraints are solved by auxiliary system and NSDF, respectively. Our proposed controller has advantages in terms of the following aspects:

1. UDE is designed to estimate the model uncertainties and external disturbance, and only the bandwidth of the unknown object is required. Furthermore, the proposed control scheme is easy to be implemented and tuned while bringing a good robust performance.
2. NSDF is designed to deal with the output constraints. Compared with BLF, using NSDF can avoid the employment of piecewise BLF when output constraints are transformed from symmetry to asymmetric.
3. Combined with NSDF and UDE, a novel task space tracking controller is first proposed for uncertain robot manipulators with input saturation and output constraints. Compared with most existing UDE-based controllers for robot manipulators without input saturation and output constraints [28, 29, 30, 31, 32], the proposed control scheme has more extensive applications.

The rest of this paper is organized as follows. Section 2 gives the problem formulation. UDE-based tracking control design, stability analysis and selection of parameters are presented in Section 3. Section 4 provides comparative simulation results and analysis. Section 5 concludes the study.

Notation: Throughout this paper, $(.)^{-1}$ denotes the inverse of a matrix, $(.)^{+}$ denotes the pseudo-inverse of a matrix. $(.)^{T}$ denotes transposition of a vector or a matrix. $\|.\|$ denotes the two-norm, $\|.\|_F$ denotes the f-norm. "$*$" denotes convolution operation. $\mathcal{L}(.)$ denotes Laplace transform operator. $\mathcal{L}^{-1}(.)$ denotes the inverse Laplace transform operator.

2. Problem Formulation

The dynamic model of an uncertain n-link rigid robot manipulator with input saturation can be described as [5, 6]

$$(M_0(q) + \Delta M_0(q))\ddot{q} + (C_0(q,\dot{q}) + \Delta C_0(q,\dot{q}))\dot{q} + (G_0(q) + \Delta G_0(q)) = U(\tau) + \tau_d \tag{1}$$

where $q, \dot{q}, \ddot{q} \in R^n$ are the link position, velocity, and acceleration vectors, respectively. $M_0(q) \in R^{n\times n}$ is the inertia matrix, which is symmetric positive definite. $C_0(q) \in R^{n\times n}$ is the Coriolis and centripetal force

https://doi.org/10.1017/S0263574722000479 Published online by Cambridge University Press

matrix. $G_0(q) \in R^n$ is the gravity vector. $\Delta M_0(q)$, $\Delta C_0(q, \dot{q})$ and $\Delta G_0(q)$ denote the modeling errors. $\tau = [\tau_1, \ldots, \tau_n]^T \in R^n$ is the input torque. $\tau_d = [\tau_{d1}, \ldots, \tau_{dn}]^T \in R^n$ denotes the bounded external disturbance. $U(\tau) = [U(\tau_1), \ldots, U(\tau_n)]^T \in R^n$ is the input saturation function vector, which can be expressed as

$$U(\tau_i) = \begin{cases} sign(\tau_i) U_{mi}, & |\tau_i| \geq U_{mi} \\ \tau_i, & |\tau_i| < U_{mi} \end{cases}, i = 1, \ldots, n \tag{2}$$

where $sign(.)$ is the standard sign function and U_{mi} is a known constant bound of $U(\tau_i)$.

Let $D = \tau_d - \Delta M_0(q)\ddot{q} - \Delta C_0(q, \dot{q})\dot{q} - \Delta G_0(q) \in R^n$ denotes the model uncertainties and bounded external disturbances, (1) can be rewritten as

$$M_0(q)\ddot{q} + C_0(q, \dot{q})\dot{q} + G_0(q) = U(\tau) + D \tag{3}$$

In task space, let $x, \dot{x}, \ddot{x} \in R^m$ denote the robot end-effector position, velocity, and acceleration vectors, respectively. Task space and joint space can be connected by

$$\dot{x} = J\dot{q} \tag{4}$$

where $J \in R^{m \times n}$ is the jacobian matrix.

Combining (3) and (4), the task space dynamic model of an uncertain n-link rigid robot manipulator is obtained:

$$M_x(x)\ddot{x} + C_x(x, \dot{x})\dot{x} + G_x(x) = J^{+T} U(\tau) + D_x \tag{5}$$

where $M_x = J^{+T} M_0 J^+$, $C_x = J^{+T}(C_0 - M_0 J^+ \dot{J})J^+$, $G_x = J^{+T} G_0$ and $D_x = J^{+T} D$.

For system (5), there are some properties as follows:

Property 1. *The inertia matrix M_x is symmetric positive definite.*

Property 2. *The matrix $\dot{M}_x - 2C_x$ is skew symmetric.*

Choosing $x_1 = x$, $x_2 = \dot{x}$, system (5) is converted to

$$\begin{cases} \dot{x}_1 = x_2 \\ \dot{x}_2 = M_x^{-1}(J^{+T} U(\tau) + D_x - C_x x_2 - G_x) \\ y = x_1 \end{cases} \tag{6}$$

where $y = [y_1, \ldots, y_m]^T$ is the system output.

For system (6), the control objective is to design an UDE-Based controller which can guarantee: the output y can track the given output y_d precisely, the control input does not violate input saturation and the output constraints are not violated, that is, $y_i(t) \in [y_i(t) \in R: -F_{i1}(t) \leq y_i(t) \leq F_{i2}(t)]$, $i = 1, \ldots, m$, where $F_{i1}(t)$ and $F_{i2}(t)$ are constraint functions.

To achieve the control objective, the following assumptions should be satisfied:

Assumption 1. *The jacobian matrix is nonsingular.*

Assumption 2. *The constraint functions $F_{i1}(t)$ and $F_{i2}(t)$ are positive, and their kth derivatives ($k = 0,1,2$) are bounded and continuous.*

Assumption 3. *The desired signal $y_d(t) = [y_{d1}(t), \ldots, y_{dm}(t)]^T$ and its jth derivatives ($j = 1,2$) are bounded. Futhermore, for any $F_{i1}(t)$ and $F_{i2}(t)$, there exist some positive constants S_{i1} and S_{i2} and functions $Y_{i1}(t)$ and $Y_{i2}(t)$ satisfying $S_{i1} \leq F_{i1}(t) - Y_{i1}(t)$ and $S_{i2} \leq F_{i2}(t) - Y_{i2}(t)$ such that $-F_{i1}(t) < -Y_{i1}(t) \leq y_{di}(t) \leq Y_{i2}(t) < F_{i2}(t)$, $i = 1, \ldots, m$.*

Remark 1. Assumption 1 is commonly used in task space tracking control of robot manipulators [33, 34, 35]. Assumption 2 is often used in studies that use NSDF to solve output or state constraints [16, 36, 37]. Assumption 3 is a common assumption about the desired signal in literature that considers time-varying output or state constraints [36, 38, 39, 40].

https://doi.org/10.1017/S0263574722000479 Published online by Cambridge University Press

3. UDE-Based Control Design

3.1. Control design

In this section, an UDE-based tracking controller is designed for uncertain robot manipulators with input saturation and output constraints. This section is divided into three steps. In step 1, we combine NSDF and backstepping method to derive the virtual control law α_1 and auxiliary variable η_1. In step 2, the control law τ and auxiliary variable η_2 are derived by combining UDE and backstepping method, and the stability of robot manipulator is proved by Lyapunov method. In step 3, we construct an auxiliary system using η_1 and η_2, and the stability of the auxiliary system is proved by Lyapunov method.

Step1: To solve the output constraints, two NSDF vectors $\zeta = [\zeta_1, \ldots, \zeta_m]^T$ and $\zeta_d = [\zeta_{d1}, \ldots, \zeta_{dm}]^T$ are defined as follows:

$$\zeta_i = K\frac{y_i(t)}{(F_{i1}(t) + y_i(t))(F_{i2}(t) - y_i(t))}, i = 1, \ldots, m \tag{7}$$

$$\zeta_{di} = K\frac{y_{di}(t)}{(F_{i1}(t) + y_{di}(t))(F_{i2}(t) - y_{di}(t))}, i = 1, \ldots, m \tag{8}$$

where K is a positive constant.

Remark 2. For the initial value $y_i(0) \in [y_i(t) \in R: -F_{i1}(t) \le y_i(t) \le F_{i2}(t)]$, we can obtain: $\zeta_i \to \pm\infty$ if and only if $y_i(t) \to -F_{i1}(t)$ or $y_i(t) \to F_{i2}(t)$. In other words, the problem of satisfying the output constraints is transformed into the problem of ensuring the boundness of ζ_i for all $t \ge 0$.

Define $e_1 = \zeta - \zeta_d$ and $v_1 = e_1 - \eta_1$ and consider the Lyapunov function $V_1 = \frac{1}{2}v_1^T v_1$. The time derivative of V_1 is:

$$\dot{V}_1 = v_1^T(\dot{\zeta} - \dot{\zeta}_d - \dot{\eta}_1) \tag{9}$$

Taking the time derivative of each term in ζ and ζ_d based on (7) and (8), we get

$$\dot{\zeta}_i = \mu_{1i}\dot{y} + \mu_{2i}, i = 1, \ldots, m \tag{10}$$

$$\dot{\zeta}_{di} = \mu_{d1i}\dot{y}_d + \mu_{d2i}, i = 1, \ldots, m \tag{11}$$

where

$$\mu_{1i} = K\frac{F_{i1}(t)F_{i2}(t) + y_i(t)^2}{(F_{i1}(t) + y_i(t))^2(F_{i2}(t) - y_i(t))^2} \tag{12}$$

$$\mu_{2i} = K\frac{(\dot{F}_{i1}(t)F_{i2}(t) + F_{i1}(t)\dot{F}_{i2}(t) + (\dot{F}_{i2}(t) - \dot{F}_{i1}(t))y_i(t))y_i(t)}{(F_{i1}(t) + y_i(t))^2(F_{i2}(t) - y_i(t))^2} \tag{13}$$

$$\mu_{d1i} = K\frac{F_{i1}(t)F_{i2}(t) + y_{di}(t)^2}{(F_{i1}(t) + y_{di}(t))^2(F_{i2}(t) - y_{di}(t))^2} \tag{14}$$

$$\mu_{d2i} = K\frac{(\dot{F}_{i1}(t)F_{i2}(t) + F_{i1}(t)\dot{F}_{i2}(t) + (\dot{F}_{i2}(t) - \dot{F}_{i1}(t))y_{di}(t))y_{di}(t)}{(F_{i1}(t) + y_{di}(t))^2(F_{i2}(t) - y_{di}(t))^2} \tag{15}$$

Then we can obtain the time derivative of ζ and ζ_d as follows:

$$\dot{\zeta} = \mu_1\dot{y}(t) + \mu_2 \tag{16}$$

$$\dot{\zeta}_d = \mu_{d1}\dot{y}_d(t) + \mu_{d2} \tag{17}$$

where $\mu_1 = diag[\mu_{11}, \ldots, \mu_{1m}] \in R^{m\times m}$, $\mu_2 = [\mu_{21}, \ldots, \mu_{2m}]^T \in R^m$, $\mu_{d1} = diag[\mu_{d11}, \ldots, \mu_{d1m}] \in R^{m\times m}$, $\mu_{d2} = [\mu_{d21}, \ldots, \mu_{d2m}]^T \in R^m$.

https://doi.org/10.1017/S0263574722000479 Published online by Cambridge University Press

Substituting (6), (16) and (17) into (9), we have

$$\begin{aligned}\dot{V}_1 &= v_1^T(\mu_1\dot{y} + \mu_2 - \mu_{d1}\dot{y}_d - \mu_{d2} - \dot{\eta}_1)\\ &= v_1^T(\mu_1\dot{x}_1 + \mu_2 - \mu_{d1}\dot{y}_d - \mu_{d2} - \dot{\eta}_1)\\ &= v_1^T(\mu_1 x_2 + \mu_2 - \mu_{d1}\dot{y}_d - \mu_{d2} - \dot{\eta}_1)\end{aligned} \tag{18}$$

Defining $e_2 = x_2 - \alpha_1$ and $v_2 = e_2 - \eta_2$, (18) can be further transformed as

$$\dot{V}_1 = v_1^T(\mu_1(v_2 + \eta_2 + \alpha_1) + \mu_2 - \mu_{d1}\dot{y}_d - \mu_{d2} - \dot{\eta}_1) \tag{19}$$

The virtual control law α_1 and auxiliary variable η_1 are chosen as

$$\alpha_1 = \mu_1^{-1}(-c_1 e_1 + \mu_{d1}\dot{y}_d - \mu_2 + \mu_{d2}) \tag{20}$$

$$\dot{\eta}_1 = -c_1\eta_1 + \mu_1\eta_2 \tag{21}$$

where c_1 is a design constant.

Substituting (20) and (21) into (19) results in

$$\dot{V}_1 = -c_1 v_1^T v_1 + v_2^T\mu_1^T v_1 \tag{22}$$

Step2: Considering the Lyapunov function $V_2 = V_1 + \frac{1}{2}v_2^T v_2$ and taking its time derivative based on (6) and (22), we have

$$\begin{aligned}\dot{V}_2 &= \dot{V}_1 + v_2^T(\dot{e}_2 - \dot{\eta}_2)\\ &= -c_1 v_1^T v_1 + v_2^T\mu_1^T v_1 + v_2^T(\dot{x}_2 - \dot{\alpha_1} - \dot{\eta}_2)\\ &= -c_1 v_1^T v_1 + v_2^T(\mu_1^T v_1 + M_x^{-1}(J^{+T}U(\tau) + D_x - C_x x_2 - G_x) - \dot{\alpha_1} - \dot{\eta}_2)\end{aligned} \tag{23}$$

where the model uncertainties and external disturbance D_x is unknown. According to (6), D_x can be denoted as

$$D_x = M_x\dot{x}_2 + C_x x_2 + G_x - J^{+T}U(\tau) \tag{24}$$

which shows that the unkown D_x can be obtained from the known system dynamics and control signal. However, in order not to have the inputs cancel out, (24) can not be subtituted to (23) directly. Assuming that the frequency range of a signal is limited, the signal can be estimated using a filter with appropriate bandwidth information, then the procedure of UDE-based control design given in ref. [8] is adopted to handle the uncertainty so that a control law is derived. Assume that $G_f(s) = diag[G_{f1}(s), \ldots, G_{fm}(s)] \in R^{m\times m}$ is a strictly proper stable filter with the unity gain and zero phase shift over the spectrum of D_x and zero gain elsewhere. Then, D_x can be estimated by

$$\begin{aligned}\hat{D}_x &= \mathcal{L}^{-1}(G_f(s)) * D_x\\ &= \mathcal{L}^{-1}(G_f(s)) * (M_x\dot{x}_2 + C_x x_2 + G_x - J^{+T}U(\tau))\end{aligned} \tag{25}$$

where $\hat{D}_x$ is the estimate of D_x. The estimation error $\tilde{D}_x$ is defined as follows:

$$\tilde{D}_x = D_x - \hat{D}_x \tag{26}$$

According to (25) and (26), the laplace transform of $\tilde{D}_x$ is represented as

$$\begin{aligned}\tilde{D}_x(s) &= D_x(s) - \hat{D}_x(s)\\ &= D_x(s)(I - G_f(s))\end{aligned} \tag{27}$$

where $\tilde{D}_x(s)$, $D_x(s)$ and $\hat{D}_x(s)$ denote the Laplace transform of $\tilde{D}_x$, D_x and $\hat{D}_x$, respectively. Taking the inverse Laplace transform of (27), there is

$$\tilde{D}_x = D_x * (I - G_f(s)) \tag{28}$$

https://doi.org/10.1017/S0263574722000479 Published online by Cambridge University Press

Since D_x is bounded and the UDE filter $G_f(s)$ is designed close to unity over the spectrum of D_x, the estimation error $\tilde{D}_x$ is bounded according to (28). Hence, it is reasonably assumed that

$$\left\|\tilde{D}_x\right\| \leq \delta_1 \tag{29}$$

where δ_1 is a positive scalar. Then we can further obtain that $\hat{D}_x$ is bounded based on (26).

According to ref. [8], $G_f(s) = diag[G_{f1}(s), \ldots, G_{fm}(s)]$ is chosen as a first-order low-pass filter.

$$G_f(s) = diag\left[\frac{1}{T_1 s+1}, \ldots, \frac{1}{T_m s+1}\right] \tag{30}$$

where $1/T_i, i = 1, \ldots, m$ denote the bandwidth of $1/(T_i s + 1)$. Although this will cause some error in the estimation, the steady-state estimation error is always zero because $G_f(0) = I$. The amplitude gain of the filter is

$$|G_{fi}(jw)| = \frac{1}{\sqrt{T_i^2 w^2 + 1}} \in (0, 1), i = 1, \ldots, m \tag{31}$$

where w is the frequency of the input signal to the filter.

Remark 3. Let $\Delta u = U(\tau) - \tau$ and $J^{+T}\Delta u = J^{+T}U(\tau) - J^{+T}\tau$, there exists a positive constant δ_2 which satisfies $\left\|J^{+T}\Delta u\right\| \leq \delta_2$ according to ref. [41].

According to Remark 3, (23) and (25) can be rewritten as

$$\dot{V}_2 = -c_1 v_1^T v_1 + v_2^T(\mu_1^T v_1 + M_x^{-1}(J^{+T}\tau + J^{+T}\Delta u + D_x - C_x x_2 - G_x) - \dot{\alpha}_1 - \dot{\eta}_2) \tag{32}$$

$$\begin{aligned}\hat{D}_x &= \mathcal{L}^{-1}(G_f(s)) * (M_x\dot{x}_2 + C_x x_2 + G_x - J^{+T}\tau - J^{+T}\Delta u) \\ &= \mathcal{L}^{-1}(G_f(s)) * (M_x\dot{x}_2 + C_x x_2 + G_x - J^{+T}\tau) - \mathcal{L}^{-1}(G_f(s)) * (J^{+T}\Delta u)\end{aligned} \tag{33}$$

The control law τ is selected as

$$J^{+T}\tau = C_x x_2 + G_x + M_x(\dot{\alpha}_1 - \mu_1^T e_1 - c_2 e_2) - \frac{\left(v_2^T M_x^{-1}\right)^T}{2r_1^2} - \mathcal{L}^{-1}(G_f(s)) * (M_x\dot{x}_2 + C_x x_2 + G_x - J^{+T}\tau) \tag{34}$$

where c_2 and r_1 are design constants.

Solving (34), we can further obtain

$$\begin{aligned}\tau = J^T &\left(\mathcal{L}^{-1}((I - G_f(s))^{-1}) * \left(C_x x_2 + G_x + M_x(\dot{\alpha}_1 - \mu_1^T e_1 - c_2 e_2) - \frac{\left(v_2^T M_x^{-1}\right)^T}{2r_1^2}\right)\right) \\ &- J^T(\mathcal{L}^{-1}((I - G_f(s))^{-1} G_f(s)) * (M_x\dot{x}_2 + C_x x_2 + G_x))\end{aligned} \tag{35}$$

The auxiliary variable η_2 is selected as

$$\dot{\eta}_2 = -c_2\eta_2 - \mu_1^T\eta_1 + M_x^{-1}J^{+T}\Delta u + M_x^{-1}\mathcal{L}^{-1}(G_f(s)) * (-J^{+T}\Delta u) \tag{36}$$

Combining (32), (33), (35) and (36), we have

$$\dot{V}_2 = -c_1 v_1^T v_1 - c_2 v_2^T v_2 + v_2^T M_x^{-1}\tilde{D}_x - \frac{v_2^T M_x^{-1}\left(v_2^T M_x^{-1}\right)^T}{2r_1^2} \tag{37}$$

According to Young's inequality, there is

$$\begin{aligned}v_2^T M_x^{-1}\tilde{D}_x &\leq \frac{v_2^T M_x^{-1}\left(v_2^T M_x^{-1}\right)^T}{2r_1^2} + \frac{r_1^2\tilde{D}_x^T\tilde{D}_x}{2} \\ &\leq \frac{v_2^T M_x^{-1}\left(v_2^T M_x^{-1}\right)^T}{2r_1^2} + \frac{r_1^2\delta_1^2}{2}\end{aligned} \tag{38}$$

https://doi.org/10.1017/S0263574722000479 Published online by Cambridge University Press

Combined with (38), (37) becomes

$$\dot{V}_2 \leq -c_1 v_1^T v_1 - c_2 v_2^T v_2 + \frac{r_1^2 \delta_1^2}{2} \tag{39}$$

Defining $\rho_1 = 2min\{c_1, c_2\}$ and $\lambda_1 = \frac{r_1^2\delta_1^2}{2}$, we can further get

$$\dot{V}_2 \leq -\rho_1 V_2 + \lambda_1 \tag{40}$$

Solving (40), we can obtain that

$$0 \leq V_2(t) \leq \frac{\lambda_1}{\rho_1} + \left(V_2(0) - \frac{\lambda_1}{\rho_1}\right) e^{-\rho_1 t} \tag{41}$$

where $V_2(0)$ is the initial value of $V_2(t)$. Based on (41), we can further get

$$lim_{t\to\infty} V_2(t) \leq \frac{\lambda_1}{\rho_1} \tag{42}$$

Step3: To solve the input saturation, an auxiliary system has been set up:

$$\begin{cases} \dot{\eta}_1 = -c_1\eta_1 + \mu_1\eta_2 \\ \dot{\eta}_2 = -c_2\eta_2 - \mu_1^T\eta_1 + M_x^{-1}J^{+T}\Delta u + M_x^{-1}\mathcal{L}^{-1}(G_f(s)) * (-J^{+T}\Delta u) \end{cases} \tag{43}$$

In order to prove the stability of system (43), a Lyapunov function $V_a = \frac{1}{2}(\eta_1^T\eta_1 + \eta_2^T\eta_2)$ is considered. Taking the time derivative of V_a, we have

$$\begin{aligned} \dot{V}_a &= \eta_1^T(-c_1\eta_1 + \mu_1\eta_2) + \eta_2^T(-c_2\eta_2 - \mu_1^T\eta_1 + M_x^{-1} + M_x^{-1}\mathcal{L}^{-1}(G_f(s)) * (-J^{+T}\Delta u)) \\ &= -c_1\eta_1^T\eta_1 - c_2\eta_2^T\eta_2 + \eta_2^T M_x^{-1}J^{+T}\Delta u + \eta_2^T M_x^{-1}\mathcal{L}^{-1}(G_f(s)) * (-J^{+T}\Delta u) \end{aligned} \tag{44}$$

Using Young's inequality, we have

$$\eta_2^T M_x^{-1}J^{+T}\Delta u \leq \frac{\eta_2^T\eta_2}{2} + \frac{(M_x^{-1}J^{+T}\Delta u)^T(M_x^{-1}J^{+T}\Delta u)}{2} \tag{45}$$

$$\eta_2^T M_x^{-1}\mathcal{L}^{-1}(G_f(s)) * (-J^{+T}\Delta u) \leq \frac{\eta_2^T\eta_2}{2} + \frac{(M_x^{-1}\mathcal{L}^{-1}(G_f(s)) * (-J^{+T}\Delta u))^T(M_x^{-1}\mathcal{L}^{-1}(G_f(s)) * (-J^{+T}\Delta u))}{2} \tag{46}$$

Combined with (45) and (46), (44) becomes

$$\begin{aligned} \dot{V}_a \leq &-c_1\eta_1^T\eta_1 - (c_2 - 1)\eta_2^T\eta_2 + \frac{(M_x^{-1}J^{+T}\Delta u)^T(M_x^{-1}J^{+T}\Delta u)}{2} \\ &+ \frac{(M_x^{-1}\mathcal{L}^{-1}(G_f(s)) * (-J^{+T}\Delta u))^T(M_x^{-1}\mathcal{L}^{-1}(G_f(s)) * (-J^{+T}\Delta u))}{2} \end{aligned} \tag{47}$$

According to cauchy inequality, for any matrix $P \in R^{m\times n}$ and vector $Q \in R^n$, the following inequality holds:

$$(PQ)^T(PQ) \leq \|P\|_F^2 \|Q\|^2 \tag{48}$$

According to (48), we have

$$\begin{aligned} (M_x^{-1}J^{+T}\Delta u)^T(M_x^{-1}J^{+T}\Delta u) &\leq \left\|M_x^{-1}\right\|_F^2 \left\|J^{+T}\Delta u\right\|^2 \\ &\leq \delta_2^2\delta_3^2 \end{aligned} \tag{49}$$

$$\begin{aligned} (M_x^{-1}\mathcal{L}^{-1}(G_f(s)) * (-J^{+T}\Delta u))^T(M_x^{-1}\mathcal{L}^{-1}(G_f(s)) * (-J^{+T}\Delta u)) &\leq \left\|M_x^{-1}\right\|_F^2 \left\|\mathcal{L}^{-1}(G_f(s)) * (-J^{+T}\Delta u)\right\|^2 \\ &\leq \delta_3^2\delta_4^2 \end{aligned} \tag{50}$$

https://doi.org/10.1017/S0263574722000479 Published online by Cambridge University Press

where δ_2 is the upper bound of $\left\|J^{+T}\Delta u\right\|$, δ_3 is the upper bound of $\left\|M_x^{-1}\right\|_F$ and δ_4 is the upper bound of $\left\|\mathcal{L}^{-1}(G_f(s)) * (-J^{+T}\Delta u)\right\|$. $\mathcal{L}^{-1}(G_f(s)) * (-J^{+T}\Delta u)$ is bounded because $J^{+T}\Delta u$ is bounded and the amplitude gain of filter (31) is bounded.

Substituting (49) and (50) into (47) yileds

$$\begin{aligned}\dot{V}_a \leq & -c_1\eta_1^T\eta_1 - (c_2-1)\eta_2^T\eta_2 \\ & + \frac{\left\|M_x^{-1}\right\|_F^2 \left\|J^{+T}\Delta u\right\|^2}{2} \\ & + \frac{\left\|M_x^{-1}\right\|_F^2 \left\|\mathcal{L}^{-1}(G_f(s)) * (J^{+T}\Delta u)\right\|^2}{2} \\ \leq & -c_1\eta_1^T\eta_1 - (c_2-1)\eta_2^T\eta_2 + \frac{(\delta_2^2+\delta_4^2)\delta_3^2}{2}\end{aligned} \tag{51}$$

Defining $\rho_2 = 2min\{c_1, (c_2-1)\}$ and $\lambda_2 = \frac{(\delta_2^2+\delta_4^2)\delta_3^2}{2}$, we can further get

$$\dot{V}_a \leq -\rho_2 V_a + \lambda_2 \tag{52}$$

Solving the inequality (52), we have

$$0 \leq V_a(t) \leq \frac{\lambda_2}{\rho_2} + \left(V_a(0) - \frac{\lambda_2}{\rho_2}\right) e^{-\rho_2 t} \tag{53}$$

where $V_a(0)$ is the initial value of $V_a(t)$. Based on (53), we can further get

$$lim_{t\to\infty} V_a(t) \leq \frac{\lambda_2}{\rho_2} \tag{54}$$

3.2. Stability analysis

Theorem 1. *Considering the robot manipulator* (1) *under Assumptions 1, 2 and 3, the virtual control law* (20), *the auxiliary system* (43) *and the proposed UDE-based control law* (35) *can guarantee that the output constraints are not violated, all signals in the closed-loop system are bounded and the tracking error converges to a small neighborhood around zero.*

Proof of Theorem 1: The proof is divided into two parts. One part proves that all signals in the closed-loop system are bounded and the output constraints are not violated. The other part proves that the tracking error converges to a small neighborhood around zero.

Part 1: The formula (41) and (53) can be scaled to

$$0 \leq V_2(t) \leq \frac{\lambda_1}{\rho_1} + V_2(0)e^{-\rho_1 t} \tag{55}$$

$$0 \leq V_a(t) \leq \frac{\lambda_2}{\rho_2} + V_a(0)e^{-\rho_2 t} \tag{56}$$

which mean that for $t \geq max\left\{0, \frac{1}{\rho_1}\ln\left(\frac{V_2(0)\rho_1}{\lambda_1}\right)\right\}$, the signals v_1 and v_2 will remain within the compact sets Ω_{v_1} and Ω_{v_2}, respectively, defined by:

$$\Omega_{v_1} := \left\{v_1 \in R^m \middle| \|v_1\| \leq 2\sqrt{\frac{\lambda_1}{\rho_1}}\right\} \tag{57}$$

$$\Omega_{v_2} := \left\{v_2 \in R^m \middle| \|v_2\| \leq 2\sqrt{\frac{\lambda_1}{\rho_1}}\right\} \tag{58}$$

https://doi.org/10.1017/S0263574722000479 Published online by Cambridge University Press

similarly, for $t \geq max\left\{0, \frac{1}{\rho_2}\ln\left(\frac{V_a(0)\rho_2}{\lambda_2}\right)\right\}$, the signals η_1 and η_2 will remain within the compact sets Ω_{η_1} and Ω_{η_2}, respectively, defined by:

$$\Omega_{\eta_1} := \left\{\eta_1 \in R^m | \, \|\eta_1\| \leq 2\sqrt{\frac{\lambda_2}{\rho_2}}\right\} \tag{59}$$

$$\Omega_{\eta_2} := \left\{\eta_2 \in R^m | \, \|\eta_2\| \leq 2\sqrt{\frac{\lambda_2}{\rho_2}}\right\} \tag{60}$$

Because v_1, v_2, η_1 and η_2 are bounded, $e_1 = v_1 + \eta_1$ and $e_2 = v_2 + \eta_2$ are bounded. According to Assumption 3 and (8), ζ_d is bounded. Then we can further derive that $\zeta = e_1 + \zeta_d$ is bounded. Based on (7) and the boundness of ζ, the system output y is bounded and the output constraints are not violated. Due to Assumption 2 and the boundness of y_i and y_{di}, it is obvious that μ_1, μ_2, μ_{d1} and μ_{d2} are bounded from (12) to (15). Furthermore, the boundness of α_1 is guaranteed from (20). Then we can derive that $x_2 = e_2 + \alpha_1$ is bounded. Finally, τ is bounded based on (35). All signals in the closed-loop system are bounded.

Part 2: Next we discuss the tracking error $e_3 = y - y_d = [e_{31}, \ldots, e_{3m}]^T$. According to (7), (8) and $e_1 = \zeta - \zeta_d$, the i th element of e_1 can be described as

$$e_{1i} = K\frac{y_i(t)}{(F_{i1}(t) + y_i(t))(F_{i2}(t) - y_i(t))} - K\frac{y_{di}(t)}{(F_{i1}(t) + y_{di}(t))(F_{i2}(t) - y_{di}(t))}, i = 1, .., m \tag{61}$$

Let $\epsilon_1 = (F_{i1}(t) + y_i(t))(F_{i2}(t) - y_i(t))(F_{i1}(t) + y_{di}(t))(F_{i2}(t) - y_{di}(t))$ and $\epsilon_2 = F_{i1}(t)F_{i2}(t) + y_i(t)y_{di}(t)$, (61) can be expressed as

$$\epsilon_1 e_{1i} = K\epsilon_2 e_{3i} \tag{62}$$

where ϵ_1 and ϵ_2 are positive and bounded based on Assumptions 2 and 3. Defining $\epsilon = \epsilon_1/(K\epsilon_2)$, (62) can be rewritten as

$$\epsilon e_{1i} = e_{3i} \tag{63}$$

Taking the absolute of (63), we can further get

$$\begin{aligned} |e_{3i}| &\leq \bar{\epsilon}|e_{1i}| \\ &\leq \bar{\epsilon}\,\|e_1\| \\ &\leq \bar{\epsilon}(\,\|v_1\| + \|\eta_1\|\,) \end{aligned} \tag{64}$$

where $\bar{\epsilon}$ is the upper bound of ϵ.

According to (57), (59) and (64), for $t \geq max\left\{0, \frac{1}{\rho_1}\ln\left(\frac{V_2(0)\rho_1}{\lambda_1}\right), \frac{1}{\rho_2}\ln\left(\frac{V_a(0)\rho_2}{\lambda_2}\right)\right\}$, the tracking error e_{3i} will remain within the compact set $\Omega_{e_{3i}}$:

$$\Omega_{e_{3i}} := \left\{e_{3i} \in R | |e_{3i}| \leq 4\bar{\epsilon}\sqrt{max\left\{\frac{\lambda_1}{\rho_1}, \frac{\lambda_2}{\rho_2}\right\}}\right\} \tag{65}$$

This completes the proof of Theorem 1.

3.3. Selection of control parameters

In order to obtain good tracking performance, the selection criteria of corresponding control parameters are given as follows:

(1) The backstepping design parameters c_1, c_2 can affect the convergent rate of tracking error. Large values of c_1 and c_2 bring faster error convergence, but the control amplitude will increase if too large

https://doi.org/10.1017/S0263574722000479 Published online by Cambridge University Press

c_1 and c_2 are chosen. The design parameter r_1 should be a small positive constant to guarantee good tracking performance. In our simulation, c_1, c_2 and r_1 are chosen as 40, 100 and 1, respectively.

(2) The design parameter K is introduced in NSDF. Increasing K value can reduce the steady-state error, but will bring large control amplitude. In our simulation, K is chosen as 0.01.

(3) The design parameters $T_i, i = 1, .., m$ in (30) should be selected small to ensure small estimation error. In our simulation, T_1 and T_2 are chosen as 0.014.

4. Simulation

To demonstrate the effectiveness and superiority of the proposed UDE-based tracking controller, simulation studies are carried out using a two-link rigid robot manipulator.

4.1. Simulation platform

Let the position of manipulator's joint $q = [q_1, q_2]^T$. Let m_i and l_i be the mass and length of link i, l_{ci} be the distance from joint $i-1$ to the center of mass of inertia of link i, and I_i be the moment of inertia of link i about axis coming out of the page passing through the center of mass of link $i, i = 1, 2$. The dynamic model of the two-link robot manipulator [14] can be described as formula (1), where

$$M_0(q) = \begin{bmatrix} M_{11} & M_{12} \\ M_{21} & M_{22} \end{bmatrix}$$

$$C_0(q, \dot{q}) = \begin{bmatrix} C_{11} & C_{12} \\ C_{21} & C_{22} \end{bmatrix}$$

$$G_0(q) = \begin{bmatrix} G_{11} \\ G_{21} \end{bmatrix}$$

and

$$M_{11} = m_1 l_{c1}^2 + m_2(l_1^2 + l_{c2}^2 + 2l_1 l_{c2} cosq_2) + I_1 + I_2$$

$$M_{12} = m_2(l_{c2}^2 + l_1 l_{c2} cosq_2) + I_2$$

$$M_{21} = m_2(l_{c2}^2 + l_1 l_{c2} cosq_2) + I_2$$

$$M_{22} = m_2 l_{c2}^2 + I_2$$

$$C_{11} = -m_2 l_1 l_{c2} \dot{q}_2 sinq_2$$

$$C_{12} = -m_2 l_1 l_{c2}(\dot{q}_1 + \dot{q}_2) sinq_2$$

$$C_{21} = m_2 l_1 l_{c2} \dot{q}_1 sinq_2$$

$$C_{22} = 0$$

$$G_{11} = (m_1 l_{c2} + m_2 l_1) g cosq_1 + m_2 l_{c2} g cos(q_1 + q_2)$$

$$G_{21} = m_2 l_{c2} g cos(q_1 + q_2)$$

The model uncertainties are given as $\Delta M_0(q) = -0.1 M_0(q)$, $\Delta C_0(q, \dot{q}) = -0.2 C_0(q, \dot{q})$, $\Delta G_0(q) = -0.1 G_0(q)$. The external disturbance is chosen as $\tau_d = [sin(t), sin(t)]^T$. $UD = [UD_1, UD_2]^T$ denotes

https://doi.org/10.1017/S0263574722000479 Published online by Cambridge University Press

Table I. *Parameters of the robot.*

Parameter	Description	Value	Unit
m_1	Mass of link 1	2.0	kg
m_2	Mass of link 2	0.85	kg
l_1	Length of link 1	0.35	m
l_2	Length of link 2	0.31	m
I_1	Inertia of link 1	0.06125	kgm^2
I_2	Inertia of link 2	0.02042	kgm^2

Table II. *Controller parameters.*

Controllers	Parameters
Proposed controller	$c_1 = 40$, $c_2 = 100$, $r_1 = 1$, K $= 0.01$, $T_1 = 0.014$, $T_2 = 0.014$
Adaptive NN controler	$K_1 = \text{diag}\,[30, 30]$,$K_2 = \text{diag}\,[110,110]$, $\Gamma_1 = \Gamma_2 = 80$,$\delta_1 = \delta_2 = 0.001$, $P_1 = \text{diag}\,[3, 3]$, $P_2 = \text{diag}\,[5, 5]$, $\lambda_\tau = \lambda_1 = \lambda_2 = 1$, $\beta = 0.1$, $L = \text{diag}\,[6, 6]$, $\overline{M}_x = \text{diag}\,[4, 4]$
IDCSMC	$k_1 = 10$, $K_p = 100$, $K_d = 20$, $K_s = 1$

model uncertainties and external disturbance. The jacobian matrix is given as follows:

$$J(q) = \begin{bmatrix} -l_1 sin(q_1) - l_2 sin(q_1 + q_2) & -l_2 sin(q_1 + q_2) \\ l_1 cos(q_1) + l_2 cos(q_1 + q_2) & l_2 cos(q_1 + q_2) \end{bmatrix}$$

The robot manipulator parameters are listed in Table I.

Then system (1) can be converted to (5) based on (4). The initial position and velocity of the robot manipulator are given as $x_1(0) = [0.235, 0.205]^T$ and $x_2(0) = [0, 0]^T$. The initial state value of auxiliary system are set to $\eta_1 = [0, 0]^T$ and $\eta_2 = [0, 0]^T$. $y = [y_1, y_2]^T$ denotes the system output. The desired trajectory is given as $y_d = [0.2sin(\pi t), 0.2cos(\pi t)]^T$. $e_3 = [e_{31}, e_{32}]^T = y - y_d$ denotes the trajectory tracking error. The output constraint functions are selected as $F_{11} = 0.21 - 0.03sin(\pi t)$, $F_{12} = 0.21 + 0.03cos(\pi t)$, $F_{21} = 0.21 - 0.03cos(\pi t + \pi/2)$ and $F_{22} = 0.21 + 0.03cos(\pi t + \pi/2)$. The input saturation values are chosen as $U_m = [U_{m1}, U_{m2}]^T = [15, 5]^T$.

To further evaluate the performance of the proposed controller, we select two comparative controllers from the literature. The adaptive NN tracking controller [41] is designed as

$$\tau_x = -\overline{M}_x(K_2 z_2 + L^{-1}\hat{w}^T\phi\left(Z) + \hat{D} - \dot{\alpha} + \vartheta_1 + P_2\vartheta_2 + z_2 \left\|\vartheta_2\right\|^2 \left\|\overline{M}_x^{-1}\right\|^4 \lambda_1\hat{\Delta}_\tau + \varphi\right)$$

and the inverse dynamics control algorithm based on the chattering-free continuous sliding-mode controller (IDCSMC) [42] is designed as

$$\tau = M_0 J^{-1}(\ddot{y}_d - \dot{J}\dot{q} + K_s s(t)) + C_0\dot{q} + G_0 - \hat{d}(t)$$

where the sliding surface vector s is defined as

$$s = K_d(\dot{y}_d(t) - \dot{y}(t)) + K_p(y_d(t) - y(t))$$

4.2. Simulation results

In this section, we present the simulation results of the proposed controller, the adaptive NN controller and IDCSMC. The controller parameters are listed in Table II. The simulation time is 20 s.

Figure 1 shows the curves of the system outputs y_1 and y_2 under the control of proposed controller, adaptive NN controller and IDCSMC, respectively. Similarly, the curves of tracking errors e_{31} and e_{32} are shown in Fig. 2. Figure 3 shows the curves of control inputs τ_1 and τ_2. The curves of UDE estimation

https://doi.org/10.1017/S0263574722000479 Published online by Cambridge University Press

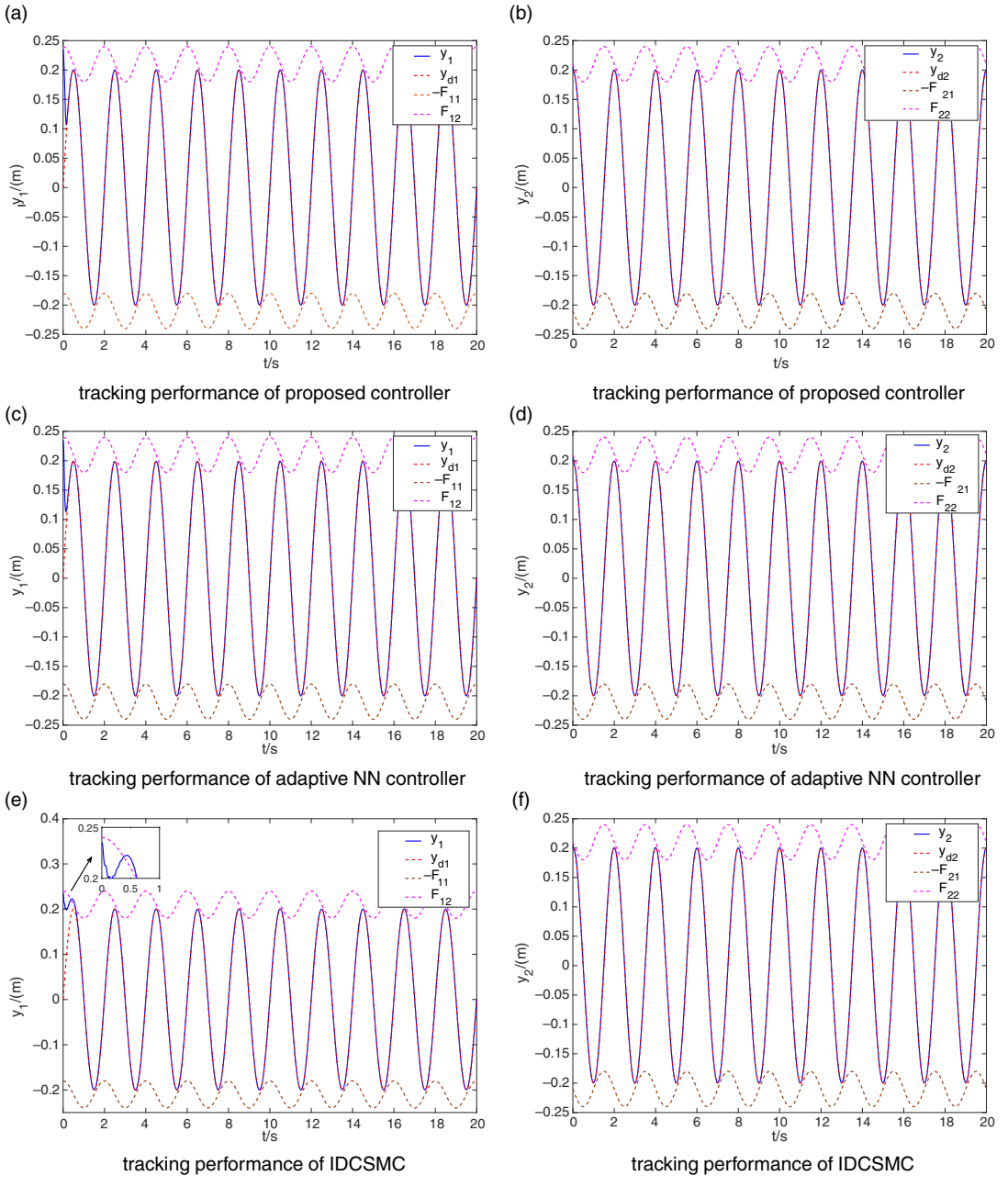

Figure 1. *Tracking performance.*

are given in Fig. 4. According to the simulation results, we can get the following conclusions. (1) All the three controllers can ensure the system output tracks on the given trajectory. (2) The proposed control achieves the smallest steady-state tracking error. (3) The proposed controller and adaptive NN controller can satisfy input saturation and output constraints, but IDCSMC can't. (4) UDE can estimate the model uncertainties and external disturbances precisely.

https://doi.org/10.1017/S0263574722000479 Published online by Cambridge University Press

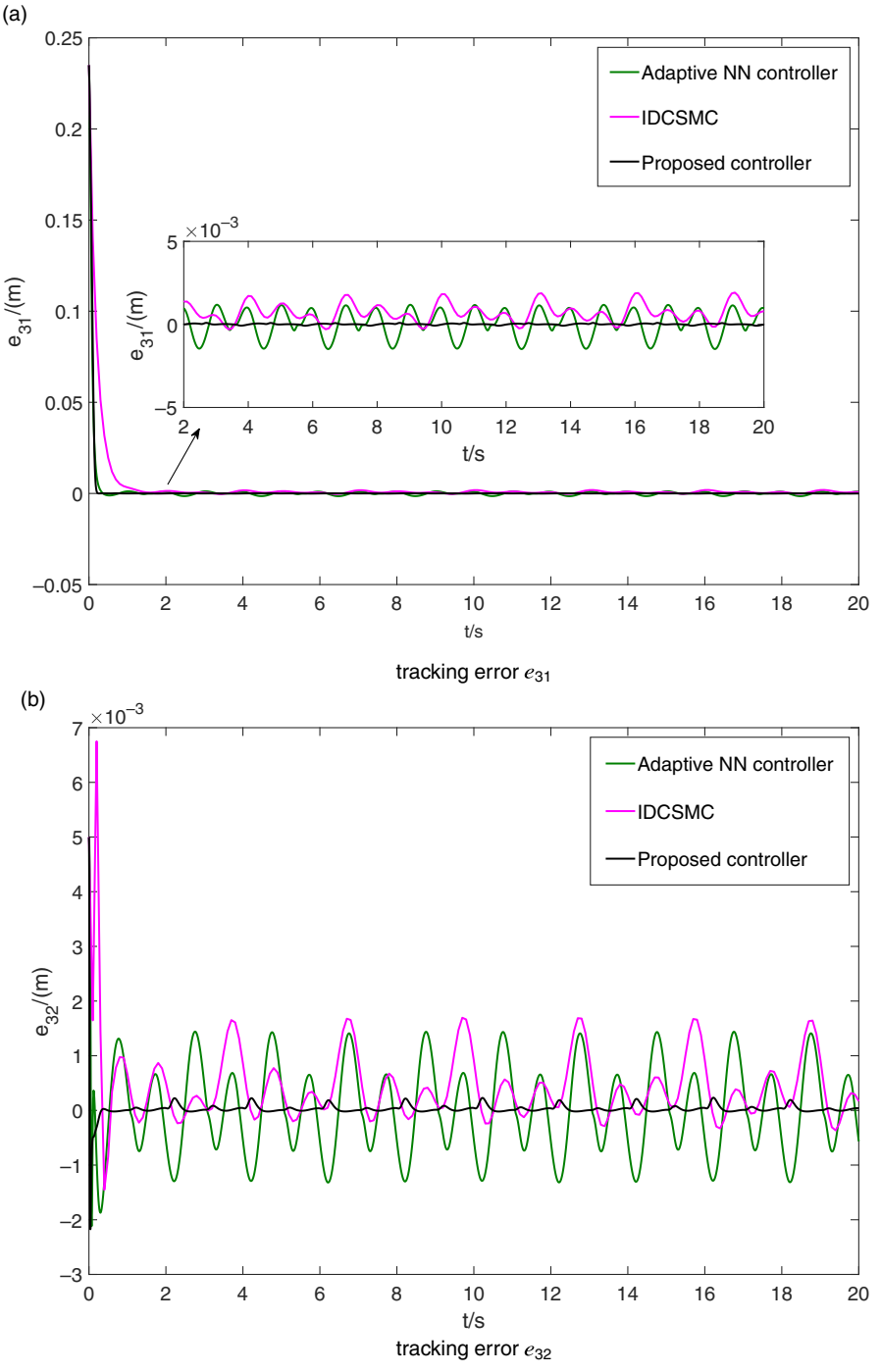

Figure 2. *Tracking error.*

https://doi.org/10.1017/S0263574722000479 Published online by Cambridge University Press

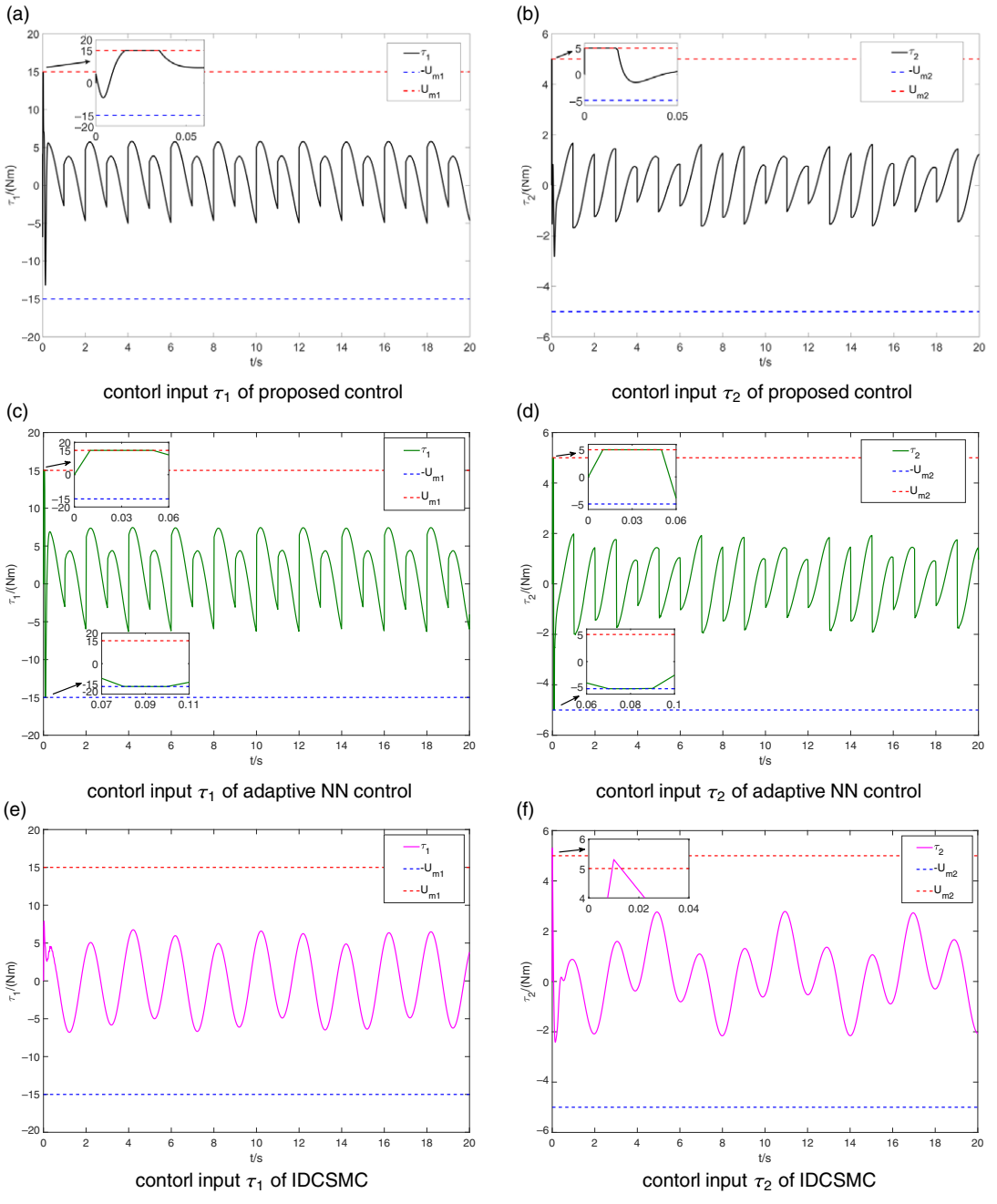

Figure 3. *Control input.*

4.3. Performance comparisons

For performance analysis, we use root mean square (RMS) and maximum (MAX) values of the sampled tracking error $e(i)$ for comparisons [43, 44], which are defined as

$$RMS(e) = \sqrt{\sum_{i=1}^{N} \frac{e^2(i)}{N}}$$

$$MAX(e) = maximum(|e|)$$

https://doi.org/10.1017/S0263574722000479 Published online by Cambridge University Press

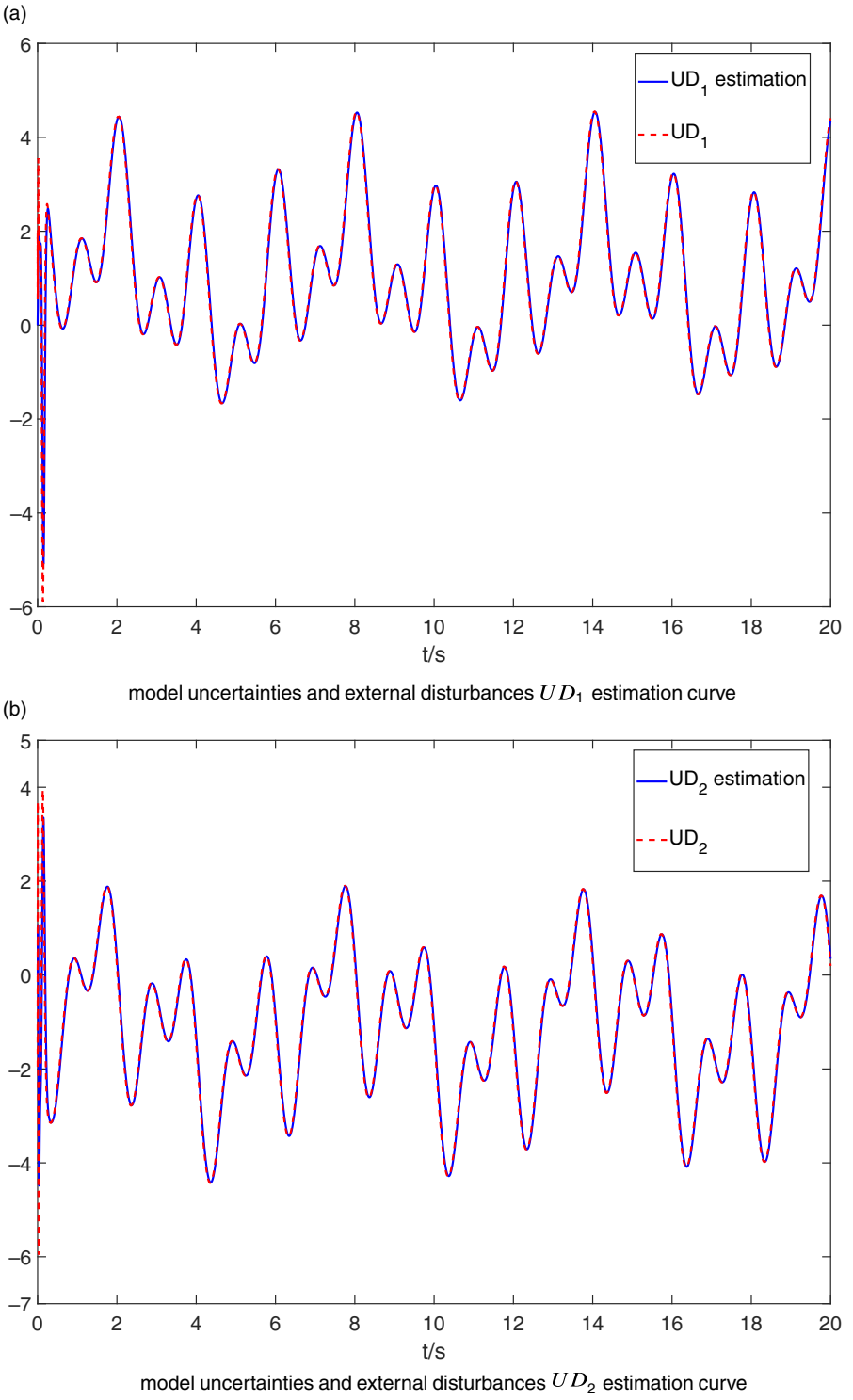

Figure 4. *Model uncertainties and external disturbances estimation curve.*

https://doi.org/10.1017/S0263574722000479 Published online by Cambridge University Press

Table III. *Performance comparisons of controllers.*

	RMS(e_{31})	**RMS(e_{32})**	**MAX(e_{31}),t > 2s**	**MAX(e_{32}),t > 2s**
Proposed controller	0.007529	0.000097	0.000093	0.000186
adaptive NN controler	0.007745	0.000804	0.001423	0.001435
IDCSMC	0.010259	0.000754	0.001818	0.001677
Improvement of proposed controller compared with adaptive NN controller	3%	88%	93%	87%
Improvement of proposed controller compared with IDCSMC	27%	87%	95%	89%

where N is the number of sampled tracking error. N is chosen as 5001 and the sample time is 0.01 s. Sampling starts at $t = 0s$. Table III shows the performance comparisons of three controllers. The proposed controller achieves the smallest RMS values for both two coordinates. In particular, the performance improvements in terms of RMS error for the proposed controller compared with the adaptive NN controller and IDCSMC are 3%, 27% for e_{31} and 88%, 87% for e_{32}, respectively. Also, when t > 2s, the performance improvements in terms of MAX error for the proposed controller compared with the adaptive NN controller and IDCSMC are 93%, 95% for e_{31} and 87%, 89% for e_{32}, respectively. The results show that the proposed control method has better robustness and tracking performance compared with the other two controllers.

5. Conclusion

An UDE-based task space tracking controller is proposed for uncertain robot manipulators with asymmetric time-varying output constraints and input saturation. Firstly, UDE is used to approximate the model uncertainties and external disturbances, and only the bandwidth of the unknown plant model is required for design. Secondly, NSDF is utilized to deal with the output constraints. Thirdly, a second order auxility system is created to solve the input saturation. Finally, the system stability and the boundness of the closed-loop signals are proved by Lyapunov stability theory. The output constraints are not violated and the control input does not violate the input saturation. Simulation results are presented to illustrate the effectiveness and superiority of the proposed control strategy.

In the furture, we tend to design an adaptive UDE-based controller for uncertain flexible joint robot in task space.

Acknowledgements. The authors thank the associate editor and anonymous reviewers for their useful comments to improve the quality of the manuscript.

Conflicts of Interest. The authors declare that they have no conflicts of interest.

Financial Support. This work is partially supported by the Guangdong Science and Technology Project under Grant Nos. 2015B010133002 and 2017B090910011.

Ethical Considerations. None.

Authors' Contributions. None.

References

[1] W. He, B. Huang, Y. Dong, Z. Li and C.-Y. Su, "Adaptive neural network control for robotic manipulators with unknown deadzone," *IEEE Trans. Cybernet*. **48**(9), 2670–2682 (2018).

[2] Q. Zhou, S. Zhao, H. Li, R. Lu and C. Wu, "Adaptive neural network tracking control for robotic manipulators with dead zone," *IEEE Trans. Neural Netw. Learn. Syst*. **30**(12), 3611–3620 (2019).

[3] S. Ling, H. Wang and P. X. Liu, "Adaptive fuzzy tracking control of flexible-joint robots based on command filtering," *IEEE Trans. Ind. Electron.* **67**(5), 4046–4055 (2020).

[4] V.-T. Nguyen, C.-Y. Lin, S.-F. Su and W. Sun, "Finite-time adaptive fuzzy tracking control design for parallel manipulators with unbounded uncertainties," *Int. J. Fuzzy Syst.* **21**(2), 545–555 (2019).

[5] D. Shi, J. Zhang, Z. Sun, G. Shen and Y. Xia, "Composite trajectory tracking control for robot manipulator with active disturbance rejection," *Control. Eng. Pract.* **106**(4), 104670 (2021).

[6] Y. Zhang, C. Hua and K. Li, "Disturbance observer-based fixed-time prescribed performance tracking control for robotic manipulator," *Int. J. Syst. Sci.* **50**(13), 2437–2448 (2019).

[7] L. Zhang, W. Qi, Y. Hu and Y. Chen, "Disturbance-observer-based fuzzy control for a robot manipulator using an EMG-driven neuromusculoskeletal model," *Complexity* **2020**, 1–10 (2020).

[8] Q.-C. Zhong and D. Rees, "Control of uncertain LTI systems based on an uncertainty and disturbance estimator," *J. Dynam. Syst. Meas. Control. Trans. ASME* **126**(4), 905–910 (2004).

[9] E. Kang, H. Qiao, J. Gao and W. Yang, "Neural network-based model predictive tracking control of an uncertain robotic manipulator with input constraints," *ISA Trans.* **109**(3), 89–101 (2021).

[10] S. Purwar, I. N. Kar and A. N. Jha, "Adaptive control of robot manipulators using fuzzy logic systems under actuator constraints," *Fuzzy Set Syst.* **152**(3), 651–664 (2005).

[11] D. Zhang, L. Kong, S. Zhang, Q. Li and Q. Fu, "Neural networks-based fixed-time control for a robot with uncertainties and input deadzone," *Neurocomputing*. **390**(5), 139–147 (2020).

[12] W. He, A. O. David, Z. Yin and C. Sun, "Neural network control of a robotic manipulator with input deadzone and output constraint," *IEEE Trans. Syst. Man Cybern. Syst*. **46**(6), 759–770 (2016).

[13] Z.-L. Tang, S. S. Ge, K. P. Tee and W. He, "Adaptive neural control for an uncertain robotic manipulator with joint space constraints," *Int. J. Control* **89**(7), 1428–1446 (2016).

[14] W. He, Y. Chen and Z. Yin, "Adaptive neural network control of an uncertain robot with Full-State constraints," *IEEE Trans. Cybern*. **46**(3), 620–629 (2016).

[15] W. He, H. Huang and S. S. Ge, "Adaptive neural network control of a robotic manipulator with Time-Varying output constraints," *IEEE Trans. Cybern*. **47**(10), 3136–3147 (2017).

[16] K. Zhao and Y. Song, "Removing the feasibility conditions imposed on tracking control designs for state-constrained strict-feedback systems," *IEEE Trans. Automat. Contr.* **64**(3), 1265–1272 (2019).

[17] C. Liu, Z. Zhao and G. Wen, "Adaptive neural network control with optimal number of hidden nodes for trajectory tracking of robot manipulators," *Neurocomputing*, **350**, 136–145 (2019).

[18] K. M. Dogan, E. Tatlicioglu, E. Zergeroglu and K. Cetin, "Learning control of robot manipulators in task space," *Asian J. Control* **20**(3), 1003–1013 (2018).

[19] X. Liang, Y. Wan and C. Zhang, "Task space trajectory tracking control of robot manipulators with uncertain kinematics and dynamics," *Math. Probl. Eng.* **2017**(1), 1–19 (2017).

[20] Z. Shuhua, Y. Xiaoping, J. Xiaoming and Z. Wenhui, "Adaptive control of space robot manipulators with task space base on neural network," *Telkomnika (Telecommun. Comput. Electron. Cont.)* **12**(2), 349–356 (2014).

[21] Y. Bouteraa, I. B. Abdallah and J. Ghommam, "Task-space region-reaching control for medical robot manipulator," *Comput. Electr. Eng.* **67**(5), 629–645 (2018).

[22] J. Liu, X. Dong, Y. Yang and H. Chen, "Trajectory Tracking Control for Uncertain Robot Manipulators with Repetitive Motions in Task Space," **In:** *Mathematical Problems in Engineering* (2021).

[23] G. Feng, "A new adaptive control algorithm for robot manipulators in task space," *IEEE Trans. Robot. Automat*. **11**(3), 457–462 (1995).

[24] Z. Xu, X. Zhou, T. Cheng, K. Sun and D. Huang, "Adaptive Task-Space Tracking for Robot Manipulators with Uncertain Kinematics and Dynamics and Without Using Acceleration," **In:** *2017 IEEE International Conference on Robotics and Biomimetics, ROBIO 2017* (Institute of Electrical and Electronics Engineers Inc., Macau, China, 2017) 2018-January, December 5, 2017.

[25] H. Wang, "Adaptive control of robot manipulators with uncertain kinematics and dynamics," *IEEE Trans. Automat. Contr.* **62**(2), 948–954 (2017).

[26] Q. Hu, L. Xu and A. Zhang, "Adaptive backstepping trajectory tracking control of robot manipulator," *J. Franklin Inst.* **349**(3), 1087–1105 (2012).

[27] G. Feng, "Robust adaptive control for robot manipulator in task space," *Automat. Contr. - World Cong.* **3**, 307–310 (1994).

[28] Y.-J. Nam, "Comparison Study of Time Delay Control (TDC) and Uncertainty and Disturbance Estimation (UDE) based Control," **In:** *16th International Conference on Control, Automation and Systems, ICCAS 2016*. vol. **0** (IEEE Computer Society, October 16, 2016) .

[29] A. Patel, R. Neelgund, A. Wathore, J. P. Kolhe, M. M. Kuber and S. E. Talole, "Robust Control of Flexible Joint Robot Manipulator," **In:** *2006 IEEE International Conference on Industrial Technology, ICIT* (Institute of Electrical and Electronics Engineers Inc., Mumbai, India 2006).

[30] J. P. Kolhe, M. Shaheed, T. S. Chandar and S. E. Talole, "Robust control of robot manipulators based on uncertainty and disturbance estimation," *Int. J. Robust Nonlin.* **23**(1), 104–122 (2013).

https://doi.org/10.1017/S0263574722000479 Published online by Cambridge University Press

[31] Z. Chu, J. Li and S. Lu, "The composite hierarchical control of multi-link multi-DOF space manipulator based on UDE and improved sliding mode control," *Proc. Inst. Mech. Eng. G J. Aerosp. Eng*. **229**(14), 2634–2645 (2015).
[32] Y. Dong and B. Ren, "UDE-Based variable impedance control of uncertain robot systems," *IEEE Trans. Syst. Man Cybernet. Syst*. **49**(12), 2487–2498 (2019).
[33] S. M. Ahmadi and M. M. Fateh, "Task-space asymptotic tracking control of robots using a direct adaptive Taylor series controller," *JVC/J. Vibr. Cont*. **24**(23), 5570–5584 (2018).
[34] A. Izadbakhsh and S. Khorashadizadeh, "Robust task-space control of robot manipulators using differential equations for uncertainty estimation," *Robotica* **35**(9), 1923–1938 (2017).
[35] R. Gholipour and M. M. Fateh, "Adaptive task-space control of robot manipulators using the Fourier series expansion without task-space velocity measurements," *Meas. J. Int. Meas. Confede.* **123**(15), 285–292 (2018).
[36] K. Zhao and Y. Song, "Neuroadaptive robotic control under time-varying asymmetric motion constraints: A feasibility-condition-free approach," *IEEE Trans. Cybern*. **50**(1), 15–24 (2020).
[37] J. Liu, C. Wang and Y. Xu, "Distributed adaptive output consensus tracking for high-order nonlinear time-varying multi-agent systems with output constraints and actuator faults," *J. Frankl. Inst.* **357**(2), 1090–1117 (2020).
[38] Y.-J. Liu, S. Lu and S. Tong, "Neural network controller design for an uncertain robot with time-varying output constraint," *IEEE Trans. Syst*. **47**(8), 2060–2068 (2017).
[39] Y.-J. Liu and S. Tong, "Barrier Lyapunov functions-based adaptive control for a class of nonlinear pure-feedback systems with full state constraints," *Automatica.* **64**(3), 70–75 (2016).
[40] Y. Wu, T. Xu and H. Mo, "Adaptive tracking control for nonlinear time-delay systems with time-varying full state constraints," *Trans. Inst. Meas. Control* **42**(12), 2178–2190 (2020).
[41] Y. Wu, R. Huang, Y. Wang and J. Wang, "Adaptive tracking control of robot manipulators with input saturation and time-varying output constraints," *Asian J. Control.* **23**(3), 1476–1489 (2021).
[42] M. F. Asar, W. M. Elawady and A. M. Sarhan, "ANFIS-based an adaptive continuous sliding-mode controller for robot manipulators in operational space," *Multibody Syst. Dynam*. **47**(2), 95–115 (2019).
[43] J. Z. etal, "Adaptive sliding mode-based lateral stability control of steer-by-wire vehicles with experimental validations," *IEEE Trans. Veh. Technol.* **69**(9), 9589–9600 (2020).
[44] L. Chen, etal, "Robust control of reaction wheel bicycle robot via adaptive integral terminal sliding mode," *Nonlinear Dynam*. **104**(3), 2291–2302 (2021).

Cite this article: Y. Wu, F. Wan, T. Xu and H. Fang (2022). "UDE-based task space tracking control of uncertain robot manipulator with input saturation and output constraint", Robotica **40**, 3651–3668. https://doi.org/10.1017/S0263574722000479